Frontiers in Bioscience Landmark

Front. Biosci. (Landmark Ed) **2026**; 31(11): 56404
https://doi.org/10.31083/FBL56404

Original Research

DL-3-n-Butylphthalide Attenuates Cisplatin-Induced Hippocampal Injury and Recognition Memory Deficits in Mice

Jing Zhang[1,†], Mengyuan Yao[1,†], Min Wen[1,2], Yuhao Xu[1], Jie Wu[1], Peng Chen[1], Benhong Zhou[1,*]

[1]Department of Pharmacy, Renmin Hospital of Wuhan University, 430060 Wuhan, Hubei, China
[2]Department of Child and Adolescent Psychiatry, Jiangsu Brain Hospital, 210008 Nanjing, Jiangsu, China
*Correspondence: benhongzh@whu.edu.cn (Benhong Zhou)
[†]These authors contributed equally.

Academic Editor: Viviana di Giacomo
Submitted: 27 July 2026 Revised: 22 September 2026 Accepted: 8 October 2026 Published: 20 November 2026

Abstract

Background: Cisplatin-associated central neurotoxicity can impair recognition memory-related performance and is accompanied by abnormalities in brain regions, including the hippocampus. Although DL-3-n-butylphthalide (NBP) has antioxidant, anti-inflammatory, and neuroprotective properties, its protective profile during repeated cisplatin exposure has not been systematically characterized. **Methods:** HT22 mouse hippocampal neuronal-like cells were co-treated with 40 μM cisplatin and noncytotoxic concentrations of NBP for 24 h, followed by assessment of cell viability, interleukin-6 (IL-6) and tumor necrosis factor-α (TNF-α) levels, and the phosphorylation of phosphoinositide 3-kinase (PI3K), protein kinase B (AKT), and cAMP response element-binding protein (CREB). A mouse model of cisplatin-induced hippocampal injury was established. Mice were assigned to a control group, a cisplatin-only (DDP) group, three cisplatin-plus-NBP groups (50, 75, or 100 mg/kg NBP), and a cisplatin-plus-donepezil group (3 mg/kg donepezil). All groups except the control group received the same cisplatin regimen. Recognition memory-related performance was evaluated using the novel object recognition test. Hippocampal histopathology, superoxide dismutase (SOD) activity, malondialdehyde (MDA) levels, markers of glial reactivity, and PI3K/AKT/CREB phosphorylation were also assessed. **Results:** Cisplatin reduced HT22 cell viability and increased IL-6 and TNF-α levels, whereas NBP improved cell viability and reduced these inflammatory mediators within a noncytotoxic concentration range. NBP attenuated cisplatin-associated histopathological and redox abnormalities in the hippocampus, reduced IBA1 expression, and was associated with partial recovery of PI3K/AKT phosphorylation, with more limited evidence for changes in CREB phosphorylation. NBP treatment also altered glial reactivity-related markers. Similar restoration of PI3K/AKT/CREB phosphorylation was observed in HT22 cells. **Conclusions:** NBP attenuated cisplatin-induced injury in HT22 cells, improved novel object discrimination, and ameliorated hippocampal histopathological and redox abnormalities in female non-tumor-bearing mice. Across the *in vitro* and *in vivo* models, NBP-associated protection was accompanied by changes in PI3K/AKT/CREB phosphorylation, with partial recovery of hippocampal PI3K/AKT phosphorylation and more limited evidence for CREB phosphorylation changes. These findings support further preclinical evaluation of NBP for cisplatin-associated neurotoxicity and identify PI3K/AKT/CREB signaling as a potential mechanistic correlate.

Keywords: DL-3-n-butylphthalide; cisplatin; hippocampus; memory; oxidative stress; neuroinflammation

1. Introduction

Cancer-related cognitive impairment (CRCI) encompasses subjective and objectively measurable changes in attention, processing speed, executive function, learning, and memory that may occur before, during, or after cancer treatment [1,2,3]. Its pathogenesis is multifactorial and reflects interactions among malignancy-related factors, host susceptibility, systemic and psychological influences, and anticancer therapy [1,2,4]. Cisplatin has been implicated in cancer treatment-related cognitive impairment [5]. Despite its antitumor efficacy, experimental studies have shown that repeated systemic cisplatin exposure can induce persistent cognitive abnormalities, together with structural and molecular alterations in the central nervous system [3,5,6,7]. Characterization of cisplatin-associated neurotoxicity and identification of strategies capable of preserving neural function are therefore important preclinical objectives.

The hippocampus has received particular attention in experimental studies of cisplatin-associated neurotoxicity, with reports of impaired adult neurogenesis, elevated inflammatory cytokines, and reduced expression of synapse-related proteins in this region [7,8]. Cisplatin exposure has been associated with mitochondrial dysfunction, oxidative stress, impaired adult neurogenesis, reduced dendritic complexity and spine density, and neuronal injury within hippocampal regions [7,8,9]. At the behavioral level, however, recognition memory is supported by a distributed neural network rather than by the hippocampus alone [10,11,12]. The perirhinal cortex plays a central role in familiarity-based discrimination of individual objects, whereas hippocampal involvement is more prominent when recogni-

Copyright: © 2026 The Author(s). Published by IMR Press.
This is an open access article under the CC BY 4.0 license.

Publisher's Note: IMR Press stays neutral with regard to jurisdictional claims in published maps and institutional affiliations.

tion incorporates contextual, spatial, associative, or relational information [10,11,12]. Accordingly, the hippocampus was selected a priori as the tissue region for histological and molecular analyses in the present study, while novel object recognition was used in parallel to assess recognition memory-related performance at the behavioral level.

Cisplatin-associated central neurotoxicity is unlikely to arise from a single pathological process. In addition to the hippocampal changes described above, studies in cisplatin-exposed mice have identified brain microvascular endothelial and microglial senescence and persistent blood–brain barrier disruption [13,14]. Among candidate signaling pathways, the phosphoinositide 3-kinase/protein kinase B/cAMP response element-binding protein (PI3K/AKT/CREB) axis is biologically relevant to neuronal survival, cellular stress adaptation, synaptic plasticity, and memory-related transcription [15,16,17]. Altered Akt/CREB/BDNF-related signaling has also been associated with hippocampal neuronal injury and cognitive abnormalities in cisplatin-exposed animals [18]. These pathological processes overlap with several biological effects previously associated with DL-3-n-butylphthalide (NBP), including attenuation of oxidative and inflammatory injury, and modulation of signaling related to neuronal survival [19,20,21]. The above observations provide a biological rationale for evaluating NBP in the context of cisplatin-associated neurotoxicity.

NBP is a lipophilic small molecule with antioxidant, anti-inflammatory, mitochondrial-protective, and pro-survival properties [19,20,21]. Previous studies have reported neuroprotective effects of NBP in experimental models of cerebral ischemia and traumatic brain injury [20,22], diabetes-associated cognitive decline, post-stroke and vascular cognitive impairment [21,23], as well as other neurological disorders. In these settings, NBP-associated protection is accompanied by attenuation of oxidative and inflammatory disturbances, preservation of neuronal and synaptic integrity, and modulation of PI3K/AKT-, AKT/CREB-, and related survival-associated signaling [19,20,21]. More directly, an *in vitro* study reported that NBP attenuated inflammatory and apoptotic changes in cisplatin-exposed PC12 cells in association with altered PI3K/AKT/CREB signaling [24]. However, findings from ischemic, metabolic, traumatic, or other neurological models do not directly establish whether NBP is protective against cisplatin-associated central neurotoxicity, and integrated evidence regarding the effects of NBP on cisplatin-associated hippocampal injury and recognition memory-related impairment remains limited.

An additional knowledge gap concerns whether NBP-associated protection during cisplatin exposure is expressed coherently across different biological levels. Previous experimental studies have investigated cisplatin-associated cognitive impairment and hippocampal changes, including neuroinflammation and impaired neurogenesis [6,7,8]. A separate *in vitro* study has examined NBP in cisplatin-exposed PC12 cells [24]. It remains unclear whether NBP-associated protection is accompanied by directionally concordant signaling changes in neuronal-like cells *in vitro* and hippocampal tissue *in vivo*. To address these gaps, the present study integrated HT22 mouse hippocampal neuronal-like cells with a repeated-cycle cisplatin-exposure mouse model and evaluated complementary cellular, histological, biochemical, glial-associated, behavioral, and signaling outcomes. Phosphorylation of PI3K, AKT, and CREB was assessed in parallel in HT22 cells and mouse hippocampal tissue to determine whether the NBP-associated protective phenotype was accompanied by corresponding changes in this candidate neuroprotective signaling axis.

Accordingly, we hypothesized that NBP would attenuate cisplatin-induced injury in HT22 cells and improve recognition memory-related performance and associated hippocampal abnormalities *in vivo*. We further examined whether these effects were accompanied by improvements in redox homeostasis, changes in glial reactivity-related markers, and partial restoration of PI3K/AKT/CREB phosphorylation. By integrating complementary *in vitro* and *in vivo* endpoints, our aim was to determine whether NBP produces a coherent, mutually supportive protective phenotype during repeated cisplatin exposure, as opposed to evaluating its effects on the basis of a single endpoint. PI3K/AKT/CREB phosphorylation was therefore examined as a candidate molecular correlate of the NBP-associated protective phenotype rather than as an established causal mechanism.

2. Materials and Methods

2.1 Reagents, Antibodies, and Cell Culture

Cisplatin (DDP; CAS No. 15663-27-1; Cat. No. HY-17394) was purchased from MedChemExpress (Monmouth Junction, NJ, USA). DL-3-n-butylphthalide (NBP; batch No. 5182109002; purity, 99.80%) was obtained from CSPC NBP Pharmaceutical Co., Ltd. (Shijiazhuang, China). Donepezil hydrochloride tablets (approval No. H20050978) were purchased from Eisai China Inc. (Suzhou, China). HT22 mouse hippocampal neuronal-like cells (Cat. No. CL-0697; Procell Life Science & Technology Co., Ltd., Wuhan, China) were maintained in high-glucose Dulbecco's modified Eagle's medium supplemented with 10% fetal bovine serum and 1% penicillin–streptomycin at 37 °C in a humidified atmosphere containing 5% CO_2. Cells were passaged at a ratio of 1:3, and logarithmically growing cultures in good condition were used for experiments. Cells were seeded in 96-well plates at 1 × 10^5 cells/mL in 100 μL of complete medium per well. Drug treatment was initiated when cell confluence reached approximately 80%. The identity of the HT22 cell line was verified by short tandem repeat (STR) profiling using an 18-locus mouse STR panel. The STR profile showed

a 96.77% match with the HT22 reference profile in the Cellosaurus database. The cells tested negative for mycoplasma contamination. HT22 cells are an immortalized neuronal-like cell line derived from the mouse hippocampus and provide a stable and reproducible *in vitro* system for drug-concentration screening and assessment of neuronal-like cell injury. This cell line has been used to investigate oxidative injury, mitochondrial dysfunction, cell death, and neuroprotection-related signaling. Importantly, previous work has directly exposed HT22 cells to cisplatin and demonstrated reductions in cell viability together with cell-cycle arrest, DNA damage, and apoptosis [25]. Accordingly, HT22 cells were used in the present study as an *in vitro* model of cisplatin-induced injury in mouse hippocampal neuronal-like cells and as a cellular system for evaluating NBP-associated protection. The use of a mouse-derived cell line also provided a complementary platform for comparing the direction of cellular injury and PI3K/AKT/CREB phosphorylation changes with those observed in mouse hippocampal tissue *in vivo*.

2.2 Cisplatin-Induced HT22 Cell Injury and NBP Treatment

HT22 cells were exposed to 0, 10, 20, 30, 40, 50, 60, 70, or 80 μM cisplatin for 24 h to establish a concentration-response relationship. Separate cultures were treated with 0, 5, 10, 25, 50, 100, 250, 500, or 1000 μM NBP alone for 24 h to define the noncytotoxic concentration range. On the basis of the concentration-screening results, HT22 cells were co-treated with 40 μM cisplatin and NBP for 24 h. NBP concentrations of 5, 10, 25, 50, and 100 μM were used for the cell viability assay, whereas concentrations of 25, 50, and 100 μM were selected for inflammatory mediator and western blot analyses.

2.3 Cell Viability and Inflammatory Mediator Assays

Cell viability was assessed using the Cell Counting Kit-8 assay according to the manufacturer's instructions (Cat. No. C6005; Suzhou Xinsimei Biotechnology Co., Ltd., Suzhou, China). Absorbance was measured at 450 nm and normalized to the untreated control group. Interleukin-6 and tumor necrosis factor-α concentrations in cell culture supernatants were measured using enzyme-linked immunosorbent assay kits (Cat. Nos. HSEK0411 and ELK1272; Boster Biological Technology Co., Ltd., Wuhan, China).

2.4 Experimental Animals and Group Allocation

All animal experiments were approved by the Laboratory Animal Ethics Committee of Renmin Hospital of Wuhan University (approval No. WDRM Animal [Welfare] 20250308D) and were conducted in accordance with institutional guidelines for the care and use of laboratory animals. The reporting of the animal experiments was guided by the ARRIVE 2.0 guidelines. The animal experiments were conducted from 1 April 2025 to 1 June 2025. All animal procedures, including the final behavioral assessment and tissue collection, were completed within the validity period of the ethics approval. Sixty 7-week-old female C57BL/6J mice (16–18 g) were purchased from Hunan SJA Laboratory Animal Co., Ltd. (Changsha, China) and acclimatized for 7 days. Mice were housed under standard conditions (22 ± 2 °C, 50%–60% relative humidity, and a 12-h light/dark cycle) with free access to food and water. Using a random-number table, mice were assigned to six groups (initial n = 10 per group): control, cisplatin (DDP; 2.3 mg/kg), low-dose NBP plus cisplatin (NBP-L; 50 mg/kg NBP), medium-dose NBP plus cisplatin (NBP-M; 75 mg/kg NBP), high-dose NBP plus cisplatin (NBP-H; 100 mg/kg NBP), and donepezil plus cisplatin (D; 3 mg/kg donepezil). The initial group size of 10 mice per group was determined before the experiment with reference to a previous study of cisplatin-induced cognitive impairment in mice [26]. No formal a priori sample size calculation was performed. Unexpected death before the scheduled endpoint was a prespecified reason for exclusion from subsequent endpoint assessments. No study-specific humane endpoints or criteria for early termination were predefined.

All 60 mice completed the treatment protocol. No unexpected deaths occurred, and no animals were excluded from their assigned endpoint assessments. According to the endpoint-allocation scheme, seven mice from each group were included in the novel object recognition (NOR) test. Among these seven mice, five animals per group were randomly selected for subsequent hippocampal superoxide dismutase (SOD) and malondialdehyde (MDA) measurements, and three of these five animals were further randomly selected for western blot analysis. Thus, the animals used for western blotting constituted a subset of those used for the SOD/MDA analyses, which in turn constituted a subset of the animals included in the behavioral assessment. The remaining three mice per group, which were not included in the behavioral assessment, were used for histopathological and immunofluorescence assessments; hematoxylin and eosin (H&E) staining and immunofluorescence were performed using tissue samples obtained from the same three animals. Selection of animals for the individual assays was independent of the observed experimental outcomes.

NBP was formulated in saline containing 0.5% Tween-80 and sonicated to obtain a uniform preparation before intraperitoneal administration. The control group received an equivalent volume of the 0.5% Tween-80/saline vehicle according to the corresponding daily administration schedule. Except for the control group, all mice received cisplatin by intraperitoneal injection at 2.3 mg/kg/day for 5 consecutive days followed by a 5-day treatment-free interval, and this cycle was repeated three times. This regimen was selected on the basis of an established repeated low-dose mouse model of cisplatin-associated cognitive impair-

ment [26]. Its cyclic structure was intended to model repeated exposure separated by recovery intervals rather than to reproduce a direct mouse-to-human dose equivalence.

NBP or donepezil was administered once daily by intraperitoneal injection at the assigned dose throughout the experimental period. Previous mouse studies have reported neuroprotective effects of intraperitoneal NBP at 50 mg/kg and 100 mg/kg in traumatic brain injury models [27,28]. Accordingly, 50 and 100 mg/kg were selected as exploratory low and high doses, respectively, and 75 mg/kg was included as an intermediate dose. On cisplatin-treatment days, NBP or donepezil was administered 1 h before cisplatin as a prespecified prophylactic schedule intended to provide drug exposure before the toxic challenge; this study was not designed to determine whether the 1-h interval was optimal. Donepezil was included as a pharmacological reference for comparison with NBP in novel object recognition performance and hippocampal injury-related outcomes. The estrous cycle of the female mice was neither monitored nor synchronized.

2.5 Behavioral Assessment

Recognition memory-related performance was assessed using the NOR test. The test was conducted in a black plastic open-field arena (50 × 50 × 30 cm) under conditions of minimal noise and dim lighting. A video camera mounted above the apparatus was connected to a video-tracking motion-analysis system (EthoVision XT 11.5; Noldus Information Technology, The Netherlands). Seven mice per group (n = 7 independent animals/group) were included in the behavioral assessment.

The NOR test consisted of three phases: habituation, training, and testing. During the habituation phase, each mouse was placed individually in the empty open-field arena and allowed to explore freely for 5 min. During the training phase, two identical objects were placed in the arena, and each mouse was allowed to explore them freely for 10 min. Twenty-four hours later, the testing phase was conducted. One of the familiar objects was replaced with a novel object, and each mouse was allowed to freely explore the familiar and novel objects for 10 min. Mouse behavior was recorded and analyzed using EthoVision XT 11.5.

Novel-object preference was quantified using the discrimination index (DI), calculated as: $DI = (T_{novel} - T_{familiar}) / (T_{novel} + T_{familiar})$, where T_{novel} and $T_{familiar}$ represent the exploration times for the novel and familiar objects, respectively.

2.6 Histopathology, Immunofluorescence, and Oxidative Stress Assays

At the designated experimental endpoint, mice were placed in an induction chamber supplied with oxygen at a flow rate of 0.5–1.0 L/min. Anesthesia was induced with 3%–4% isoflurane. Once stable anesthesia had been achieved, the isoflurane concentration was increased to 5% for euthanasia. Following respiratory arrest, exposure to 5% isoflurane was continued for at least 10 min until complete cessation of cardiac activity was confirmed. Hippocampal tissue collection was performed only after death had been confirmed. Because isoflurane was delivered by inhalation, exposure was specified by vapor concentration and oxygen flow rate rather than an injectable mg/kg dose.

Hippocampal tissue was collected after completion of behavioral testing. Three independent mice per group (n = 3/group) were used for histopathological and immunofluorescence assessments. Hematoxylin and eosin staining was used to evaluate tissue morphology in the dentate gyrus and CA3 regions. Double immunofluorescence staining for CD68 (ABclonal, Cat. No. A23738, 1:200), IBA1 (ABclonal, Cat. No. A19776, 1:2000), C3 (ABclonal, Cat. No. A26249, 1:200), and GFAP (ABclonal, Cat. No. A19058, 1:2000) was used for qualitative assessment of microglial- and astrocytic-associated reactivity, respectively. Nuclei were counterstained with Hoechst or DAPI, and all images were acquired using identical fluorescence exposure settings. Hippocampal oxidative status was assessed in five independent animals per group (n = 5/group). Superoxide dismutase (SOD) activity and malondialdehyde (MDA) levels were measured using a SOD assay kit (Cat. No. A001-3) and an MDA assay kit (Cat. No. A003-1), respectively (Nanjing Jiancheng Bioengineering Institute, Nanjing, Jiangsu, China), according to the manufacturer's instructions. Results were normalized to total protein content.

2.7 Western Blotting

Total protein was extracted from HT22 cells or mouse hippocampal tissue using radioimmunoprecipitation assay (RIPA) lysis buffer (Servicebio, Wuhan, China), and protein concentrations were determined using the bicinchoninic acid assay. Protein samples (30–50 µg per lane) were separated by 10% or 12% SDS-PAGE and transferred to polyvinylidene difluoride membranes. After blocking with 5% nonfat milk, membranes were incubated overnight at 4 °C with primary antibodies against p-PI3K (1:1000, Cat. No. YP-Ab-14485; Youpin Biotechnology), PI3K (1:1000, Cat. No. YP-Ab-14915; Youpin Biotechnology), p-AKT (1:1000, Cat. No. AP1208; Abmart), AKT (1:1000, Cat. No. A18120; Abmart), p-CREB (1:1000, Cat. No. AP1421; Abmart), CREB (1:1000, Cat. No. 12208-1-AP; Proteintech), IBA1 (1:1000, Cat. No. A19776; ABclonal), and β-actin or GAPDH (1:2000, Cat. No. GB11001-100, Cat. No. GB23303; Servicebio). Membranes were then incubated with horseradish peroxidase-conjugated goat anti-rabbit secondary antibody (1:5000, Cat. No. G2009-100ML; Servicebio) for 2 h at room temperature. Signals were detected using a chemiluminescence imaging system and quantified with ImageJ software (version 1.53e; National Institutes of Health, Bethesda, MD, USA). Phosphorylated proteins were normalized to their corresponding total proteins, and IBA1 (1:1000, Cat. No. A19776; AB-

clonal) was normalized to the indicated loading control. For mouse hippocampal western blot analysis, three animals per group were randomly selected from the same five animals used for the SOD and MDA analyses. Thus, the reported n = 3 represents three independent biological replicates from three individual animals per experimental group rather than technical replicates.

2.8 Statistical Analysis

Data are presented as mean ± SEM. Statistical analyses were performed using SPSS version 27.0 (SPSS Inc., Chicago, IL, USA) and GraphPad Prism version 9.5 (GraphPad Software, San Diego, CA, USA). Normality of ANOVA residuals and homogeneity of variance were assessed using the Shapiro–Wilk and Brown–Forsythe tests, respectively. Homogeneity of variance was satisfied for all analyzed endpoints, and residuals were generally compatible with normality, except for the IL-6 endpoint, which was interpreted with caution. For the IL-6 endpoint, which did not meet the residual normality assumption, the ANOVA-based results were obtained as exploratory findings. Overall group effects were assessed using ordinary one-way ANOVA including all experimental groups. In intervention experiments, the CON–DDP comparison was tested as a single planned linear contrast within the full ANOVA model (CON = 1, DDP = −1, and all treatment groups = 0), using the pooled residual variance from that model. Treatment effects were assessed in a separate one-way ANOVA model including only the DDP and treatment groups, with Dunnett-adjusted comparisons against DDP as the common reference. In concentration-screening experiments, Dunnett's test was used to compare each concentration with the 0 μM control. For the novel object recognition test, DI values were additionally compared with the theoretical chance level of zero using two-sided one-sample *t* tests with Holm correction across groups. Eta squared (η^2) was reported for omnibus one-way ANOVA. All tests were two-sided, and $p < 0.05$ was considered statistically significant.

3. Results

3.1 NBP Improves Cell Viability and Reduces Inflammatory Mediator Levels in Cisplatin-Treated HT22 Cells

Cisplatin reduced HT22 cell viability in a concentration-dependent manner, with significant reductions observed from 10 μM onward (Fig. 1A). At 40 μM, cell viability was reduced to approximately 54% of the untreated control, whereas higher concentrations caused more severe loss of viability. Therefore, 40 μM cisplatin was selected for subsequent experiments. NBP alone did not significantly affect cell viability at 5–100 μM, whereas 250–1000 μM significantly reduced viability (Fig. 1B). Thus, 5–100 μM was considered a noncytotoxic concentration range under the present experimental conditions. In cisplatin-treated cells, 25, 50, and 100 μM NBP significantly increased cell viability compared with the DDP group, whereas 5 and 10 μM NBP showed no significant effect (Fig. 1C). Cisplatin also significantly increased IL-6 and tumor necrosis factor-α (TNF-α) levels compared with the CON group. High-dose NBP significantly reduced IL-6 levels, whereas the low- and medium-dose groups did not reach statistical significance (Fig. 1D). In contrast, all three NBP concentrations significantly reduced TNF-α levels relative to DDP (Fig. 1E). Collectively, these findings indicate that NBP attenuated cisplatin-induced HT22 cell injury and was accompanied by reductions in inflammatory mediators.

3.2 NBP-Associated Cytoprotection Is Accompanied by Partial Restoration of PI3K/AKT/CREB Phosphorylation in Cisplatin-Treated HT22 Cells

To determine whether NBP-associated cytoprotection was accompanied by changes in PI3K/AKT/CREB signaling, the phosphorylation levels of PI3K, AKT, and CREB were assessed by western blotting. Cisplatin significantly reduced the p-PI3K/PI3K ratio compared with the CON group. Compared with DDP, NBP-L and NBP-H significantly increased the p-PI3K/PI3K ratio, whereas NBP-M showed no significant difference (Fig. 2B). Similarly, cisplatin significantly reduced the p-AKT/AKT ratio. NBP-M and NBP-H significantly increased the p-AKT/AKT ratio relative to DDP, whereas the effect of NBP-L was not statistically significant (Fig. 2C). Cisplatin also significantly reduced the p-CREB/CREB ratio, while all three NBP concentrations significantly increased this ratio compared with DDP (Fig. 2D). Collectively, these findings indicate that NBP-associated cytoprotection was accompanied by partial restoration of PI3K/AKT/CREB phosphorylation in cisplatin-treated HT22 cells, although the response pattern varied across signaling proteins and NBP concentrations. Representative western blot images are shown in Fig. 2A.

3.3 NBP Attenuates Novel Object Recognition Deficits in Cisplatin-Treated Mice

In the novel object recognition test, cisplatin significantly reduced the DI compared with the CON group, indicating impaired novel-object discrimination. Compared with DDP, the DI was significantly higher in the NBP-H and donepezil groups, whereas no significant differences were observed in the NBP-L or NBP-M groups (Fig. 3A). When DI values were compared with the theoretical chance level of zero, only the CON group remained significantly above chance after Holm correction. The NBP-H group showed a positive mean DI, but this did not reach statistical significance relative to chance. Total object exploration time did not differ significantly among groups (Fig. 3B), suggesting that the observed DI differences were unlikely to be explained by major differences in overall object exploration. Collectively, these findings indicate that high-dose NBP attenuated cisplatin-associated impairment in novel-object discrimination.

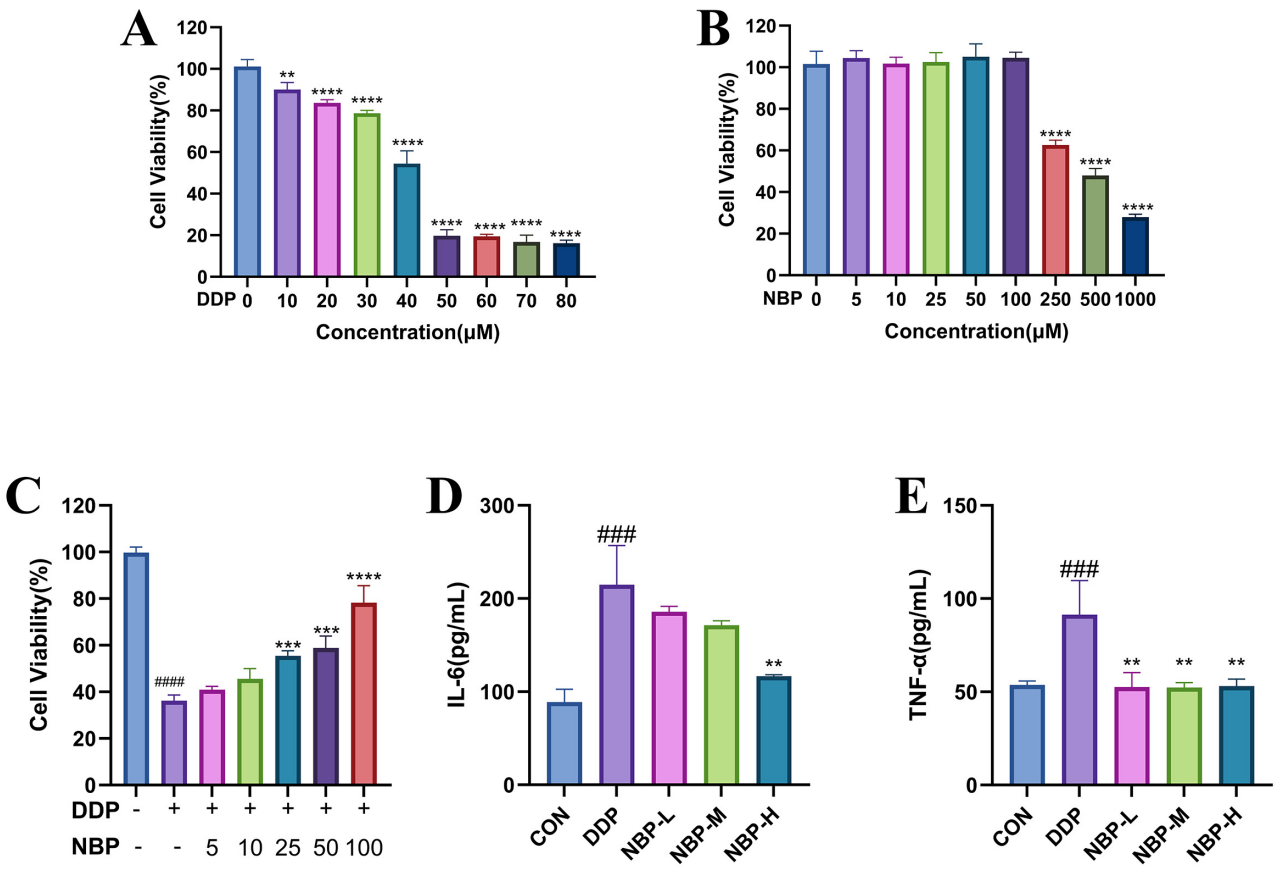


Fig. 1. NBP improved cell viability and reduced inflammatory mediator levels in cisplatin-treated HT22 cells. (A) Effect of cisplatin on HT22 cell viability after 24 h of exposure (one-way ANOVA, F(8,18) = 397.613, n = 3, $p < 0.0001$, $\eta^2 = 0.9944$). Dunnett's multiple-comparison test was performed using 0 μM cisplatin as the reference (10 μM, adjusted $p = 0.0022$; 20–80 μM, all adjusted $p < 0.0001$). (B) Effect of NBP alone on HT22 cell viability after 24 h of exposure (one-way ANOVA, F(8,18) = 166.779, n = 3, $p < 0.0001$, $\eta^2 = 0.9867$). Dunnett's multiple-comparison test was performed using 0 μM NBP as the reference (5 μM, adjusted $p = 0.9320$; 10 μM, adjusted $p > 0.9999$; 25 μM, adjusted $p = 0.9999$; 50 μM, adjusted $p = 0.8516$; 100 μM, adjusted $p = 0.9161$; 250–1000 μM, all adjusted $p < 0.0001$). (C) Effect of NBP on cell viability in cisplatin-treated HT22 cells (one-way ANOVA, F(6,14) = 91.370, n = 3, $p < 0.0001$, $\eta^2 = 0.9751$). The planned CON–DDP linear contrast within the full ANOVA model was significant ($p < 0.0001$). NBP-treated groups were compared with the DDP group using Dunnett's multiple-comparison test (5 μM, adjusted $p = 0.5537$; 10 μM, adjusted $p = 0.0778$; 25 μM, adjusted $p = 0.0007$; 50 μM, adjusted $p = 0.0001$; 100 μM, adjusted $p < 0.0001$). (D) IL-6 levels in culture supernatants (one-way ANOVA, F(4,10) = 20.069, n = 3, $p < 0.0001$, $\eta^2 = 0.8892$). The planned CON–DDP linear contrast within the full ANOVA model was significant ($p < 0.0001$). NBP-treated groups were compared with the DDP group using Dunnett's multiple-comparison test (NBP-L, adjusted $p = 0.2896$; NBP-M, adjusted $p = 0.0870$; NBP-H, adjusted $p = 0.0013$). The IL-6 residuals did not meet the normality assumption. An exact two-sided Mann–Whitney sensitivity analysis of DDP versus NBP-H was not significant (unadjusted $p = 0.10$). Significance symbols in panel (D) represent the ANOVA-based comparisons only. (E) TNF-α levels in culture supernatants (one-way ANOVA, F(4,10) = 10.718, n = 3, $p = 0.0012$, $\eta^2 = 0.8109$). The planned CON–DDP linear contrast within the full ANOVA model was significant ($p = 0.0005$). NBP-treated groups were compared with the DDP group using Dunnett's multiple-comparison test (NBP-L, adjusted $p = 0.0040$; NBP-M, adjusted $p = 0.0041$; NBP-H, adjusted $p = 0.0044$). Data are presented as mean ± SEM. Hash symbols indicate the CON–DDP model comparison, whereas asterisks indicate Dunnett-adjusted comparisons with the corresponding reference group. $^{**}p < 0.01$, $^{***}p < 0.001$, $^{****}p < 0.0001$; $\#\#\#p < 0.001$, $\#\#\#\#p < 0.0001$. NBP, DL-3-n-butylphthalide; TNF-α, tumor necrosis factor-α; DDP, cisplatin; ANOVA, analysis of variance.

3.4 Representative Hippocampal H&E Morphology and Quantitative Indices of Oxidative Status

Representative H&E-stained sections showed relatively preserved cellular organization in the dentate gyrus and CA3 regions of CON mice, whereas DDP-treated mice exhibited more disorganized cellular arrangement and looser tissue architecture. NBP-treated mice showed relatively better-preserved hippocampal morphology compared

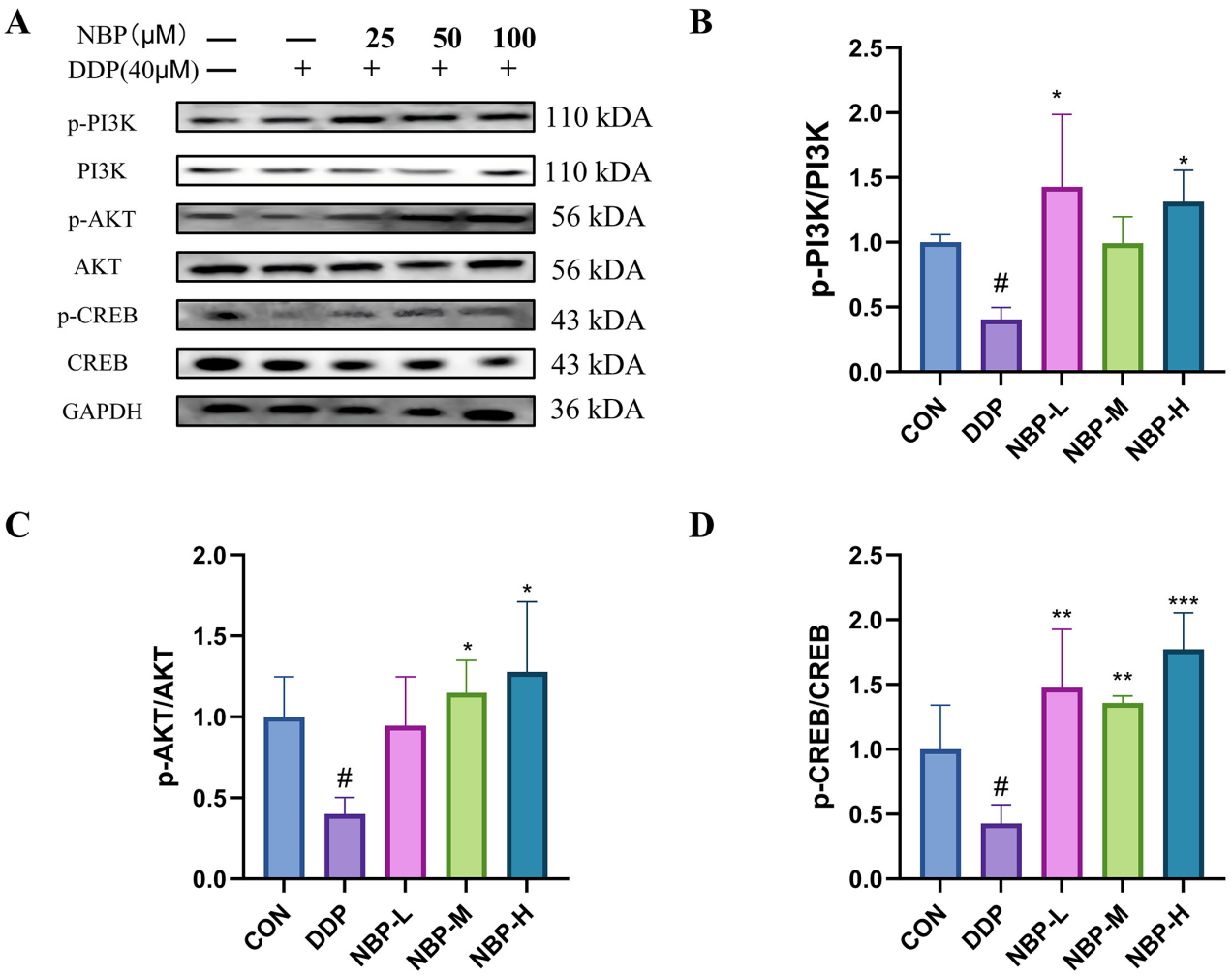


Fig. 2. The cytoprotective phenotype associated with NBP was accompanied by partial restoration of PI3K/AKT/CREB phosphorylation in cisplatin-treated HT22 cells. (A) Representative western blot bands. (B) Quantification of the p-PI3K/PI3K ratio (one-way ANOVA, F(4,10) = 5.585, n = 3, $p = 0.0126$, $\eta^2 = 0.6908$). The planned CON–DDP linear contrast within the full ANOVA model was significant ($p = 0.0314$). NBP-treated groups were compared with DDP using Dunnett's multiple-comparison test (NBP-L, adjusted $p = 0.0121$; NBP-M, adjusted $p = 0.1326$; NBP-H, adjusted $p = 0.0223$). (C) Quantification of the p-AKT/AKT ratio (one-way ANOVA, F(4,10) = 4.338, n = 3, $p = 0.0272$, $\eta^2 = 0.6344$). The planned CON–DDP linear contrast within the full ANOVA model was significant ($p = 0.0252$). Dunnett-adjusted comparisons with DDP were as follows: NBP-L, $p = 0.1126$; NBP-M, $p = 0.0312$; and NBP-H, $p = 0.0141$. (D) Quantification of the p-CREB/CREB ratio (one-way ANOVA, F(4,10) = 9.455, n = 3, $p = 0.0020$, $\eta^2 = 0.7909$). The planned CON–DDP linear contrast within the full ANOVA model was significant ($p = 0.0366$). Dunnett-adjusted comparisons with DDP were as follows: NBP-L, $p = 0.0043$; NBP-M, $p = 0.0084$; and NBP-H, $p = 0.0008$. Data are presented as mean ± SEM. Hash symbols indicate the CON–DDP model comparison, whereas asterisks indicate Dunnett-adjusted comparisons with DDP. *$p < 0.05$, **$p < 0.01$, ***$p < 0.001$; #$p < 0.05$. PI3K, phosphoinositide 3-kinase; AKT, protein kinase B; CREB, cAMP response element-binding protein.

with the DDP group (Fig. 4A). Cisplatin significantly reduced hippocampal SOD activity compared with the CON group. High-dose NBP and donepezil significantly increased SOD activity relative to DDP, whereas the NBP-L and NBP-M groups showed no significant differences (Fig. 4B). For MDA, although the overall group effect did not reach statistical significance, the model comparison showed significantly higher MDA levels in the DDP group than in the CON group. High-dose NBP significantly reduced MDA levels compared with DDP, whereas the NBP-L, NBP-M, and donepezil groups did not reach statistical significance (Fig. 4C). Collectively, these findings suggest that high-dose NBP attenuated cisplatin-associated hippocampal morphological abnormalities and was accompanied by improvement in selected indices of oxidative balance.

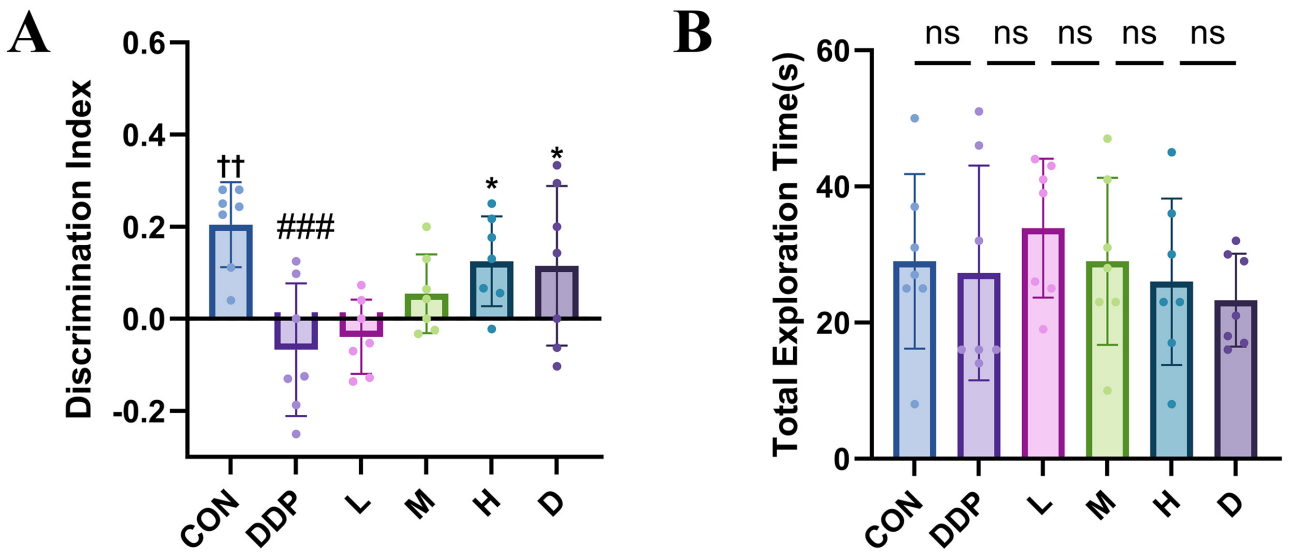


Fig. 3. NBP attenuated novel object recognition deficits in cisplatin-treated mice. (A) Discrimination index (DI) in the novel object recognition test (one-way ANOVA, F(5,36) = 5.432, n = 7, $p = 0.0008$, $\eta^2 = 0.4300$). The planned CON–DDP linear contrast within the full ANOVA model was significant ($p = 0.0001$). Treatment groups were compared with DDP using Dunnett's multiple-comparison test (NBP-L, adjusted $p = 0.9685$; NBP-M, adjusted $p = 0.2086$; NBP-H, adjusted $p = 0.0207$; donepezil, adjusted $p = 0.0299$). DI values were additionally compared with the theoretical chance level of zero using two-sided one-sample t tests with Holm correction; only the CON group remained significantly above chance (adjusted $p = 0.0066$). (B) Total object exploration time during the novel object recognition test (one-way ANOVA, F(5,36) = 0.612, n = 7, $p = 0.6913$, $\eta^2 = 0.0783$). No significant differences were observed among groups. Data are presented as mean ± SEM. Hash symbols indicate the CON–DDP model comparison, asterisks indicate Dunnett-adjusted comparisons with DDP, and dagger symbols indicate comparisons with the theoretical chance level of zero. *$p < 0.05$; ###$p < 0.001$ vs CON; ††$p < 0.01$ vs chance level. ns, not significant.

3.5 Representative Immunofluorescence Patterns of Hippocampal Glial Markers and Quantitative Analysis of IBA1 Protein Expression

Representative C3/GFAP and CD68/IBA1 double-immunofluorescence images were used to illustrate hippocampal glial marker staining patterns (Fig. 5A,B). Because these images were evaluated qualitatively and no animal-level quantitative analysis of fluorescence intensity, positive cell number, morphology, or colocalization was performed, no statistical between-group comparisons were made. Hippocampal IBA1 protein expression was quantitatively assessed by western blotting. Cisplatin significantly increased IBA1 expression compared with the CON group. Compared with DDP, IBA1 expression was significantly lower in the NBP-H and donepezil groups, whereas no significant differences were observed in the NBP-L or NBP-M groups (Fig. 5C,D). These findings indicate that high-dose NBP was associated with reduced hippocampal IBA1 expression during cisplatin exposure, while the immunofluorescence findings should be interpreted as qualitative changes in glial marker patterns rather than evidence of altered glial cell number, morphology, or functional state.

3.6 The Hippocampal Protective Phenotype Associated With NBP Is Accompanied by Partial Restoration of PI3K/AKT Phosphorylation, With More Limited Evidence for CREB Phosphorylation Changes

Representative western blot images of hippocampal PI3K, AKT, and CREB proteins are shown in Fig. 6A. Cisplatin significantly reduced the hippocampal p-PI3K/PI3K ratio compared with the CON group. Compared with DDP, NBP-M, NBP-H, and donepezil significantly increased the p-PI3K/PI3K ratio, whereas NBP-L showed no significant effect (Fig. 6B). Similarly, cisplatin significantly reduced the p-AKT/AKT ratio. NBP-M and donepezil significantly increased the p-AKT/AKT ratio relative to DDP, whereas no significant differences were observed in the NBP-L or NBP-H groups (Fig. 6C). For p-CREB/CREB, the overall group effect was not statistically significant. However, the p-CREB/CREB ratio was significantly lower in the DDP group than in the CON group in the model comparison. Compared with DDP, NBP-H significantly increased the p-CREB/CREB ratio, whereas no significant differences were observed in the NBP-L, NBP-M, or donepezil groups (Fig. 6D). Collectively, these findings indicate that NBP treatment was associated with partial restoration of hippocampal PI3K/AKT phosphorylation, with more limited evidence for CREB phosphorylation changes.

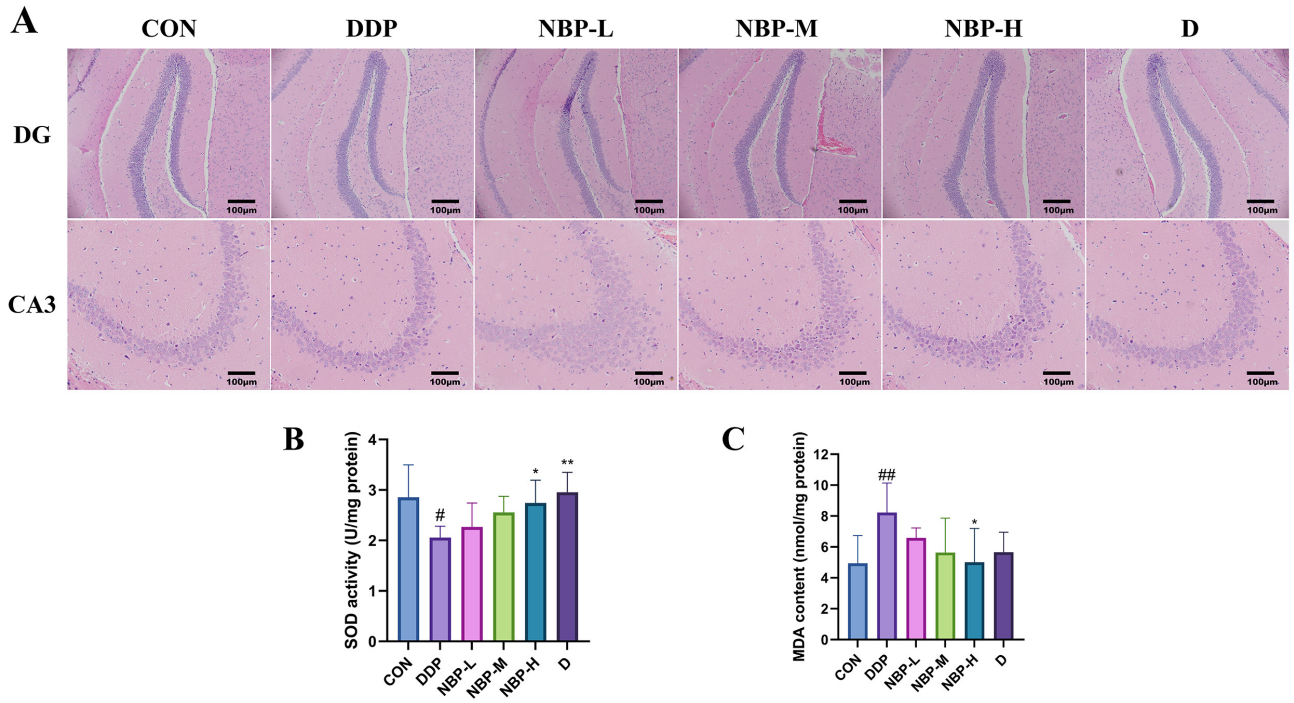


Fig. 4. Representative hippocampal H&E morphology and quantitative indices of oxidative status. (A) Representative hematoxylin and eosin-stained images of the dentate gyrus and CA3 regions. Scale bars: 100 μm. (B) Hippocampal superoxide dismutase (SOD) activity (one-way ANOVA, F(5,24) = 3.196, n = 5, $p = 0.0237$, $\eta^2 = 0.3997$). The planned CON–DDP linear contrast within the full ANOVA model was significant ($p = 0.0082$). Treatment groups were compared with DDP using Dunnett's multiple-comparison test (NBP-L, adjusted $p = 0.7996$; NBP-M, adjusted $p = 0.1600$; NBP-H, adjusted $p = 0.0350$; donepezil, adjusted $p = 0.0051$). (C) Hippocampal malondialdehyde (MDA) levels (one-way ANOVA, F(5,24) = 2.462, n = 5, $p = 0.0617$, $\eta^2 = 0.3391$). Although the overall group effect did not reach statistical significance, the planned CON–DDP linear contrast within the full ANOVA model was significant ($p = 0.0070$). Treatment groups were compared with DDP using Dunnett's multiple-comparison test (NBP-L, adjusted $p = 0.4086$; NBP-M, adjusted $p = 0.0961$; NBP-H, adjusted $p = 0.0299$; donepezil, adjusted $p = 0.0987$). Data are presented as mean ± SEM. Hash symbols indicate the CON–DDP model comparison, whereas asterisks indicate Dunnett-adjusted comparisons with DDP. *$p < 0.05$, **$p < 0.01$; #$p < 0.05$; ##$p < 0.01$.

4. Discussion

Using complementary HT22 mouse hippocampal neuronal-like cells and a repeated cisplatin-exposure mouse model, the present study evaluated the protective profile of DL-3-n-butylphthalide (NBP) across cellular, behavioral, histopathological, redox-related, glial-associated, and signaling outcomes. Cisplatin reduced HT22 cell viability and increased IL-6 and TNF-α levels *in vitro*. In female mice, cisplatin impaired novel-object discrimination and was accompanied by hippocampal histopathological abnormalities, disturbed redox homeostasis, changes in glial reactivity-related markers, and reduced PI3K/AKT phosphorylation, with more limited evidence for CREB phosphorylation changes. NBP attenuated HT22 cell injury, improved novel-object discrimination, and attenuated several of the accompanying hippocampal abnormalities. The concordant changes observed across these *in vitro* and *in vivo* models support the induction of a multi-level protective phenotype by NBP during cisplatin exposure.

Recognition memory is supported by a distributed neural network rather than by the hippocampus alone. The perirhinal cortex plays a central role in familiarity-based discrimination of individual objects and in distinguishing novel from previously encountered stimuli, whereas the hippocampus contributes more prominently when recognition incorporates contextual, spatial, associative, or relational information [10,11,12]. Accordingly, the novel object recognition findings in the present study are interpreted as changes in recognition-memory performance at the behavioral level. The hippocampus was selected a priori for histological and molecular analyses because of its well-documented vulnerability to chemotherapy-associated cognitive injury, including alterations in neurogenesis, oxidative and inflammatory homeostasis, synaptic plasticity, and neurotrophic signaling [29,30]. In cisplatin models, hippocampal neuronal abnormalities have also been associated with dysregulation of Akt/CREB/BDNF-related pro-survival and neuroplasticity signaling [18]. Thus, the concurrent improvement in novel-object discrimination and at-

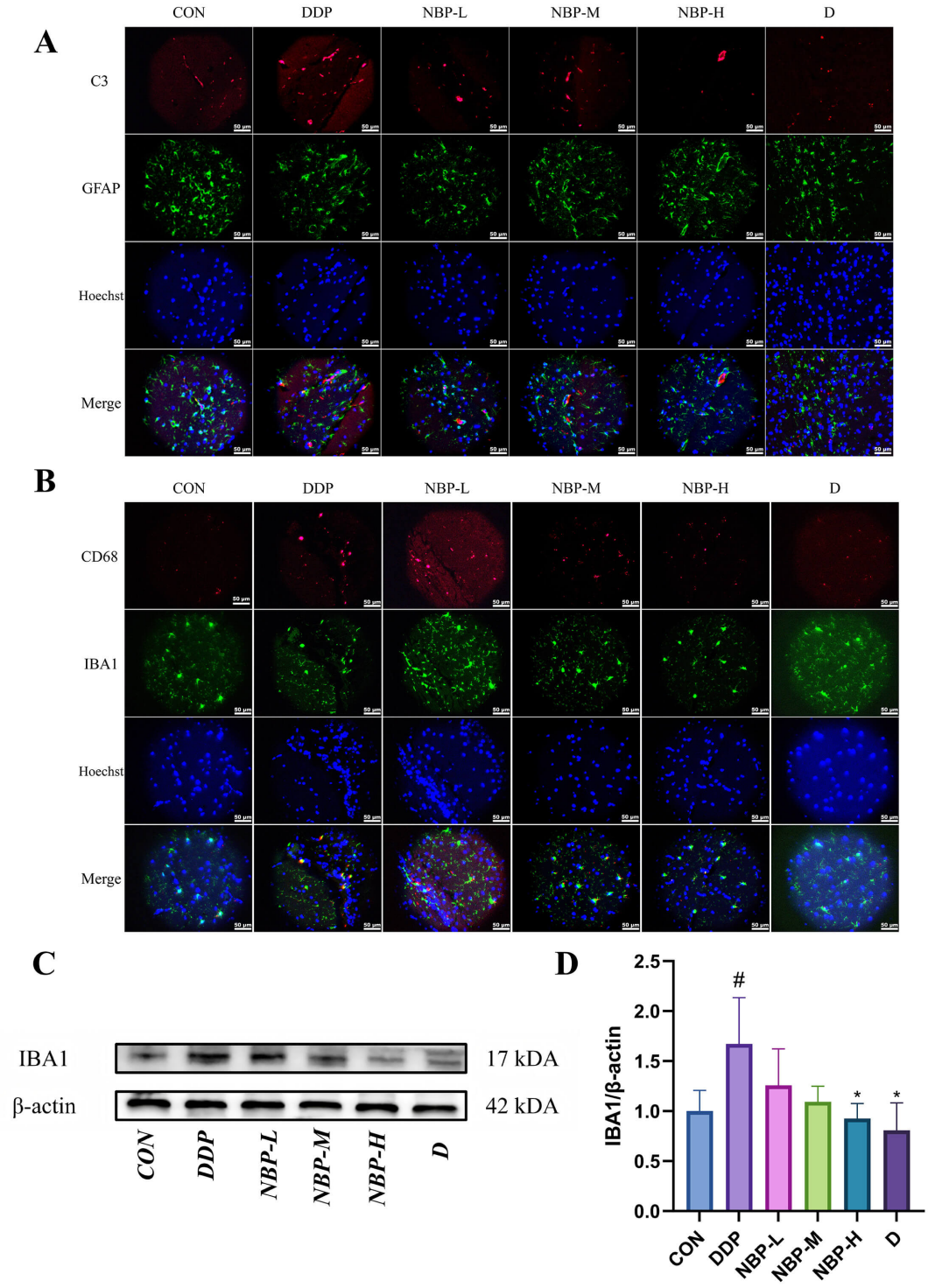


Fig. 5. Representative immunofluorescence patterns of hippocampal glial markers and quantitative analysis of IBA1 protein expression. (A) Representative C3/GFAP double-immunofluorescence images. Scale bars: 50 µm. (B) Representative CD68/IBA1 double-immunofluorescence images. Scale bars: 50 µm. (C) Representative IBA1 western blot bands. (D) Quantification of hippocampal IBA1 protein expression (one-way ANOVA, $F(5,12) = 3.342$, $n = 3$, $p = 0.0403$, $\eta^2 = 0.5820$). The planned CON–DDP linear contrast within the full ANOVA model was significant ($p = 0.0154$). Treatment groups were compared with DDP using Dunnett's multiple-comparison test (NBP-L, adjusted $p = 0.3332$; NBP-M, adjusted $p = 0.1247$; NBP-H, adjusted $p = 0.0427$; donepezil, adjusted $p = 0.0195$). Data are presented as mean ± SEM. Hash symbols indicate the CON–DDP model comparison, whereas asterisks indicate Dunnett-adjusted comparisons with DDP. *$p < 0.05$; #$p < 0.05$. C3, complement component 3; GFAP, glial fibrillary acidic protein; CD68, cluster of differentiation 68; IBA1, ionized calcium-binding adapter molecule 1.

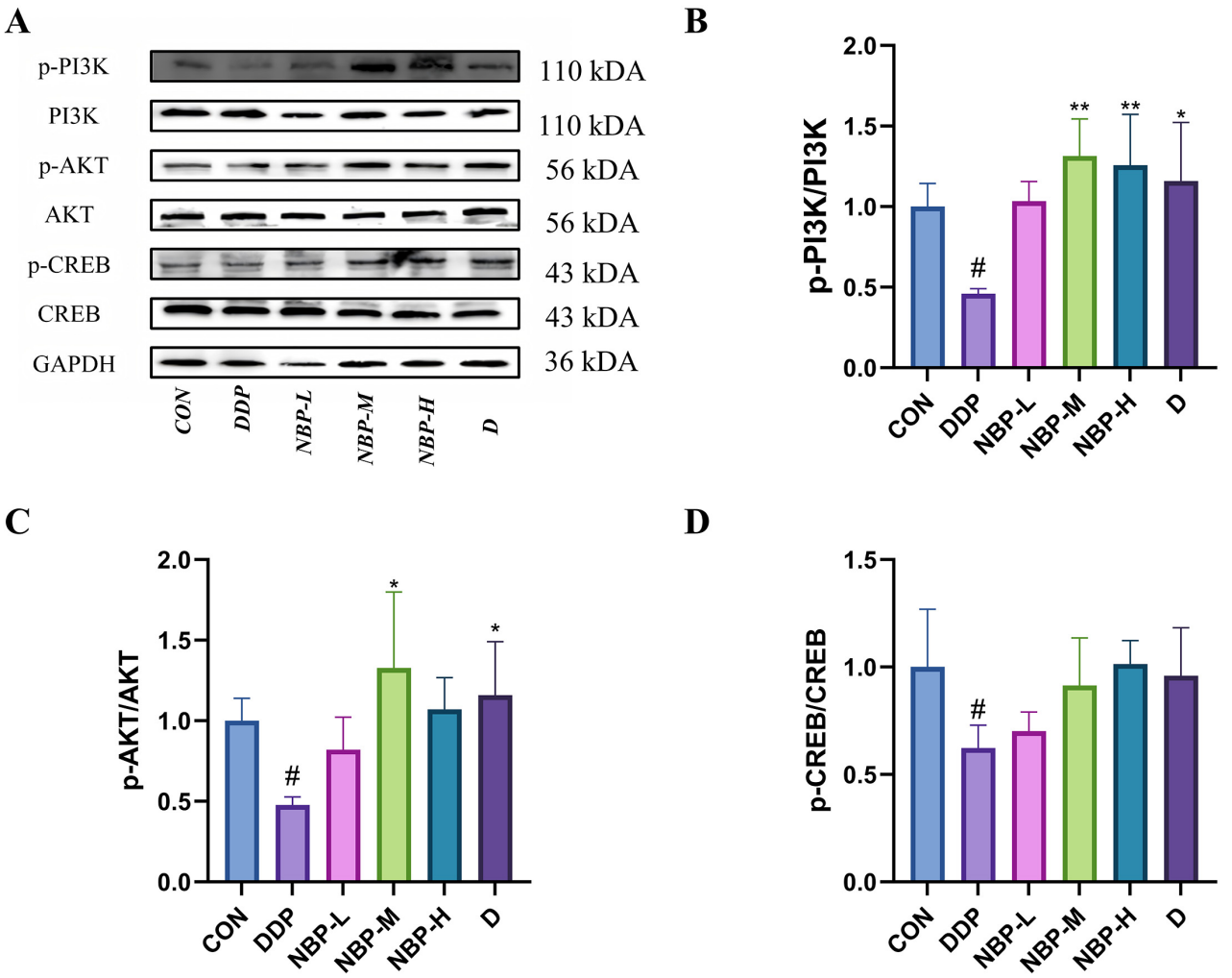


Fig. 6. The hippocampal protective phenotype associated with NBP was accompanied by partial restoration of PI3K/AKT phosphorylation, with more limited evidence for CREB phosphorylation changes. (A) Representative western blot bands. (B) Quantification of the hippocampal p-PI3K/PI3K ratio (one-way ANOVA, $F(5,12) = 5.318$, $n = 3$, $p = 0.0083$, $\eta^2 = 0.6890$). The planned CON–DDP linear contrast within the full ANOVA model was significant ($p = 0.0144$). Treatment groups were compared with DDP using Dunnett's multiple-comparison test (NBP-L, adjusted $p = 0.0516$; NBP-M, adjusted $p = 0.0055$; NBP-H, adjusted $p = 0.0085$; donepezil, adjusted $p = 0.0188$). (C) Quantification of the hippocampal p-AKT/AKT ratio (one-way ANOVA, $F(5,12) = 3.648$, $n = 3$, $p = 0.0308$, $\eta^2 = 0.6032$). The planned CON–DDP linear contrast within the full ANOVA model was significant ($p = 0.0348$). Dunnett-adjusted comparisons with DDP were as follows: NBP-L, $p = 0.4362$; NBP-M, $p = 0.0153$; NBP-H, $p = 0.0909$; and donepezil, $p = 0.0491$. (D) Quantification of the hippocampal p-CREB/CREB ratio (one-way ANOVA, $F(5,12) = 2.433$, $n = 3$, $p = 0.0961$, $\eta^2 = 0.5034$). Although the overall group effect did not reach statistical significance, the planned CON–DDP linear contrast within the full ANOVA model was significant ($p = 0.0272$). Treatment groups were compared with DDP using Dunnett's multiple-comparison test (NBP-L, adjusted $p = 0.9292$; NBP-M, adjusted $p = 0.1487$; NBP-H, adjusted $p = 0.0436$; donepezil, adjusted $p = 0.0865$). Data are presented as mean ± SEM. Hash symbols indicate the CON–DDP model comparison, whereas asterisks indicate Dunnett-adjusted comparisons with DDP. *$p < 0.05$, **$p < 0.01$; #$p < 0.05$.

tenuation of hippocampal abnormalities after NBP treatment represent complementary behavioral and regional neurobiological findings within a broader recognition-memory network. Parallel examination of the perirhinal cortex and other recognition-memory-related regions should further clarify the regional distribution of cisplatin-associated neural alterations and NBP responsiveness.

Redox imbalance was a prominent component of the hippocampal phenotype associated with cisplatin exposure. Cisplatin reduced SOD activity and increased MDA levels, consistent with impaired antioxidant capacity and enhanced lipid peroxidation. NBP increased SOD activity and reduced MDA levels, indicating that its protective phenotype was accompanied by improvement in hippocampal

redox homeostasis. This pattern is consistent with previous experimental studies in which NBP-associated neuroprotection was accompanied by attenuation of oxidative injury and regulation of antioxidant signaling, including Nrf2/HO-1-related responses [31,32]. It also concurs with broader evidence for the antioxidant and anti-inflammatory actions of NBP [31,32]. Oxidative and inflammatory disturbances within the hippocampus have likewise been implicated in chemotherapy-associated neural and cognitive abnormalities [29,30,33]. These observations extend the redox-related profile of NBP to a cisplatin-exposure setting, while SOD and MDA should be regarded as selected indices of redox status rather than providing a comprehensive assessment of oxidative injury.

Changes in glial reactivity-related markers are another component of the hippocampal response reported in experimental chemotherapy-associated cognitive impairment [34]. Astrocytes and microglia display substantial context-dependent and phenotypic heterogeneity, and alterations in individual markers do not necessarily correspond to a defined activation or functional state [35,36,37]. In the present study, C3/GFAP and CD68/IBA1 double-immunofluorescence staining provided qualitative and representative observations of spatial staining patterns, whereas hippocampal IBA1 protein expression was quantitatively assessed by Western blot. NBP treatment was accompanied by changes in glial reactivity-related markers, while quantitative Western blot analysis showed attenuation of the cisplatin-associated increase in hippocampal IBA1 expression. Therefore, these findings are most appropriately interpreted as marker-associated glial changes rather than as evidence that NBP directly suppresses microglial or astrocytic activation. Quantitative assessment of GFAP, C3, and CD68, together with analyses of cell number, morphology, spatial distribution, colocalization, and additional functional markers will be required to characterize these glial responses more comprehensively.

The PI3K/AKT/CREB signaling axis provides a plausible molecular correlate linking the cellular and hippocampal findings. PI3K/AKT signaling contributes to neuronal survival, metabolic homeostasis, and cellular stress adaptation, whereas CREB-dependent transcription participates in synaptic plasticity and memory-related gene regulation [15,16,17]. Altered Akt/CREB/BDNF-related signaling was previously associated with cisplatin-induced hippocampal neuronal injury and cognitive abnormalities [18]. In HT22 cells, cisplatin significantly reduced p-PI3K/PI3K, p-AKT/AKT, and p-CREB/CREB ratios, and NBP treatment increased these phosphorylation indices in a dose- and endpoint-dependent manner. In hippocampal tissue, cisplatin was associated with significant reductions in p-PI3K/PI3K, p-AKT/AKT, and p-CREB/CREB in the model comparisons. NBP treatment was associated with partial recovery of these phosphorylation indices, although the pattern varied across proteins and doses. In particular, the overall group effect for hippocampal p-CREB/CREB was not significant, and the CREB finding should therefore be interpreted more cautiously than the PI3K and AKT results. Further pathway-directed pharmacological or genetic studies will be required to define its functional contribution.

The present findings are broadly consistent with the established multitarget neuroprotective profile of NBP [38,39,40]. Previous studies have associated NBP with attenuation of oxidative and inflammatory injury [31,32,40], preservation of blood-brain barrier integrity and synaptic plasticity [21,41], and modulation of pro-survival signaling [42] in ischemic, metabolic, hypoperfusion, and neurodegenerative models. The present study extends this experimental profile to repeated cisplatin exposure by integrating neuronal-like cell injury and inflammatory mediators with recognition-memory performance and selected hippocampal histopathological, redox, glial-associated, and signaling outcomes within the same experimental framework. The principal contribution of the present work therefore lies in providing evidence that the protective profile associated with NBP extends across complementary cellular and *in vivo* settings in a cisplatin-related neurotoxicity model, with PI3K/AKT/CREB phosphorylation representing a shared candidate molecular correlate across these experimental systems.

The timing of NBP administration is important for interpreting the protective profile observed here. NBP was administered before cisplatin on cisplatin-treatment days and continued throughout the experimental period. The present design therefore primarily evaluates prophylactic or protective intervention during repeated cisplatin exposure rather than treatment after neurotoxicity has become established. Whether NBP can reverse neuronal, hippocampal, or behavioral abnormalities after cisplatin-associated injury has developed remains to be determined. Future studies that directly compare preventive and post-injury treatment paradigms may help to define the therapeutic time window of NBP.

While the use of female mice provides a sex-defined experimental context, the applicability of these findings to male animals remains to be established. Sex may influence the neural and cognitive consequences of cisplatin exposure [43], and the present study was not designed to evaluate sex-by-treatment interactions. Furthermore, the estrous cycle was not monitored or synchronized. Studies incorporating adequately powered male and female cohorts, together with estrous-stage assessment when biologically relevant, should help to determine whether cisplatin toxicity and NBP responsiveness are influenced by sex-related biological factors.

The non-tumor-bearing design of this study provided a controlled setting for evaluating cisplatin-associated neural injury without the additional cognitive, inflammatory, and metabolic influences associated with tumor burden. However, cisplatin is clinically administered in the context of

malignancy, where tumor biology, systemic host responses, chemotherapy, and nervous-system effects can interact. The NBP-associated protective effects observed here were demonstrated in HT22 neuronal-like cells and hippocampal tissue from non-tumor-bearing mice, and therefore their relevance to tumor cells remains unresolved. This distinction is particularly important because PI3K/AKT signaling regulates survival responses in both neural and malignant cells [15,44]. Accordingly, the partial restoration of PI3K/AKT/CREB phosphorylation observed here should be regarded as a candidate molecular correlate of the neural protective phenotype rather than evidence of neural selectivity or an established causal mechanism.

Preclinical evidence also suggests that the biological effects of NBP may depend on the cellular and pathological context. Antiproliferative activity of NBP has been reported in lung cancer cells and a xenograft model [45], whereas NBP has been shown to activate PI3K/AKT-related signaling in non-neural endothelial tissues and cells [46]. These observations highlight the need to assess neuroprotection and antitumor efficacy within the same oncological setting. Future studies using syngeneic tumor models or human tumor xenografts should evaluate cognitive and hippocampal outcomes in parallel with tumor growth, tumor burden, tumor-cell proliferation and apoptosis, intratumoral PI3K/AKT signaling, and cisplatin responsiveness. Complementary studies in cisplatin-sensitive and cisplatin-resistant tumor cells from different tumor origins may further clarify whether NBP modifies cisplatin sensitivity in a context-dependent manner. Such integrated studies will be essential in determining whether the neuroprotective profile of NBP can be maintained without compromising the antitumor activity of cisplatin, and for defining its translational potential during cisplatin-based chemotherapy.

Overall, the present findings indicate that NBP-associated protection during cisplatin exposure extends from HT22 neuronal-like cells to behavioral and hippocampal outcomes in female non-tumor-bearing mice. Improvement in novel-object discrimination occurred in parallel with attenuation of hippocampal histopathological and redox abnormalities, changes in glial reactivity-related markers, and partial restoration of PI3K/AKT/CREB phosphorylation. The cross-level concordance of these findings provides a basis for further preclinical investigation of NBP in cisplatin-associated neurotoxicity and supports PI3K/AKT/CREB signaling as a candidate molecular correlate of the NBP protective phenotype.

5. Limitations

Several limitations should be considered when interpreting the present findings. First, HT22 cells are immortalized mouse hippocampal neuronal-like cells and do not reproduce the cellular complexity of primary hippocampal neurons or neuron–glia interactions *in vivo*. Second, behavioral assessment was based on novel object recognition; although the perirhinal cortex is central to object-familiarity discrimination and the hippocampus contributes to contextual and associative aspects of recognition memory, the present study analyzed hippocampal tissue only and did not perform parallel regional analyses. Third, selected biochemical and molecular endpoints were evaluated with relatively small biological sample sizes, and the immunofluorescence observations were qualitative rather than animal-level quantitative measurements. Fourth, only female mice were studied and the estrous cycle was not monitored. Fifth, systemic cisplatin toxicity was not evaluated in the present study; therefore, the potential contribution of systemic toxicity to the observed behavioral and hippocampal changes cannot be excluded. Sixth, the prophylactic timing of NBP administration addresses protection during cisplatin exposure rather than treatment of established neurotoxicity. Finally, the non-tumor-bearing model does not address the effect of NBP on tumor-cell responses or cisplatin antitumor efficacy, and the PI3K/AKT/CREB findings represent signaling associations that require pathway-directed validation.

6. Conclusions

In conclusion, prophylactic NBP attenuated cisplatin-associated injury in HT22 neuronal-like cells and improved novel-object discrimination in female mice, accompanied by partial amelioration of hippocampal morphological and redox abnormalities. NBP-associated protection was accompanied by reduced hippocampal IBA1 expression and partial recovery of PI3K/AKT-related phosphorylation, with more limited evidence for CREB phosphorylation changes, supporting this signaling axis as a candidate molecular correlate rather than an established causal mechanism. These findings provide a basis for further investigation of NBP as a potential neuroprotective strategy during cisplatin exposure, particularly in tumor-bearing models that simultaneously evaluate neuroprotection and cisplatin antitumor efficacy.

Abbreviations

AKT, protein kinase B; ANOVA, analysis of variance; C3, complement component 3; CRCI, cancer-related cognitive impairment; CREB, cAMP response element-binding protein; DAPI, 4′,6-diamidino-2-phenylindole; DDP, cisplatin; DG, dentate gyrus; GFAP, glial fibrillary acidic protein; IBA1, ionized calcium-binding adapter molecule 1; IL-6, interleukin-6; MDA, malondialdehyde; NBP, DL-3-n-butylphthalide; PI3K, phosphoinositide 3-kinase; SEM, standard error of the mean; SOD, superoxide dismutase; TNF-α, tumor necrosis factor-α.

Availability of Data and Materials

The data supporting the findings of this study are available from the corresponding author upon reasonable request.

Author Contributions

JZ: Methodology, Formal analysis, Data curation, Writing – original draft, Writing – review & editing. MYY: Methodology, Formal analysis, Data curation, Project administration, Writing – review & editing. MW: Data curation, Formal analysis, Writing – review & editing. YHX: Investigation, Project administration, Writing – review & editing. JW: Methodology, Investigation, Writing – review & editing. PC: Investigation, Formal analysis, Writing – review & editing. BHZ: Conceptualization, Methodology, Funding acquisition, Writing – review & editing. All authors contributed to editorial changes in the manuscript. All authors read and approved the final manuscript. All authors have participated sufficiently in the work and agreed to be accountable for all aspects of the work.

Ethics Approval and Consent to Participate

All animal procedures were approved by the Laboratory Animal Ethics Committee of Renmin Hospital of Wuhan University (approval No. WDRM Animal [Welfare] 20250308D). Animal care and experimental procedures followed the Chinese national standard Laboratory animals—General code of animal welfare (GB/T 42011-2022), and the ethical review followed Laboratory animal—Guideline for ethical review of animal welfare (GB/T 35892-2018). The reporting of the animal experiments was guided by the ARRIVE 2.0 guidelines. Consent to participate was not applicable because the study did not involve human participants.

Acknowledgment

The authors gratefully acknowledge the Central Laboratory and Animal Facility of Renmin Hospital of Wuhan University for providing technical support, equipment, and experimental facilities.

Funding

This study was funded by CSPC NBP Pharmaceutical Co., Ltd. (Grant No. YXSY-2023-05), which also provided the DL-3-n-butylphthalide used in this study free of charge. The authors declare that they have no other conflicts of interest with the sponsoring company that could affect the objectivity of the present study.

Conflicts of Interest

The authors disclose that CSPC NBP Pharmaceutical Co., Ltd. provided financial support for this study and supplied DL-3-n-butylphthalide free of charge. The authors declare that they have no other conflicts of interest with the sponsoring company that could affect the objectivity of the present study.

Supplementary Material

Supplementary material associated with this article can be found, in the online version, at https://doi.org/10.31083/FBL56404.

References

[1] Demos-Davies K, Lawrence J, Seelig D. Cancer related cognitive impairment: a downside of cancer treatment. Frontiers in Oncology. 2024; 14: 1387251. https://doi.org/10.3389/fonc.2024.1387251

[2] Fleming B, Edison P, Kenny L. Cognitive impairment after cancer treatment: mechanisms, clinical characterization, and management. BMJ (Clinical Research Ed.). 2023; 380: e071726. https://doi.org/10.1136/bmj-2022-071726

[3] Schagen SB, Tsvetkov AS, Compter A, Wefel JS. Cognitive adverse effects of chemotherapy and immunotherapy: are interventions within reach? Nature Reviews. Neurology. 2022; 18: 173–185. https://doi.org/10.1038/s41582-021-00617-2

[4] Yang Y, Von Ah D. Cancer-related cognitive impairment: updates to treatment, the need for more evidence, and impact on quality of life-a narrative review. Annals of Palliative Medicine. 2024; 13: 1265–1280. https://doi.org/10.21037/apm-24-70

[5] Kim HG, Rashid MA, Poleschuk M, Ullah F, Lee SH, Kim SH, et al. Cognitive dysfunction in chemobrain: Molecular mechanisms and therapeutic implications. Biomedicine & Pharmacotherapy = Biomedecine & Pharmacotherapie. 2025; 192: 118581. https://doi.org/10.1016/j.biopha.2025.118581

[6] Squillace S, Niehoff ML, Doyle TM, Green M, Esposito E, Cuzzocrea S, et al. Sphingosine-1-phosphate receptor 1 activation in the central nervous system drives cisplatin-induced cognitive impairment. The Journal of Clinical Investigation. 2022; 132: e157738. https://doi.org/10.1172/JCI157738

[7] Oliveros A, Yoo KH, Rashid MA, Corujo-Ramirez A, Hur B, Sung J, et al. Adenosine A2A receptor blockade prevents cisplatin-induced impairments in neurogenesis and cognitive function. Proceedings of the National Academy of Sciences of the United States of America. 2022; 119: e2206415119. https://doi.org/10.1073/pnas.2206415119

[8] Park SH, Ko JR, Han J. Exercise alleviates cisplatin-induced toxicity in the hippocampus of mice by inhibiting neuroinflammation and improving synaptic plasticity. The Korean Journal of Physiology & Pharmacology: Official Journal of the Korean Physiological Society and the Korean Society of Pharmacology. 2024; 28: 145–152. https://doi.org/10.4196/kjpp.2024.28.2.145

[9] Qutifan S, Saleh T, Abu Shahin N, ELBeltagy M, Obeidat F, Qattan D, et al. Melatonin mitigates cisplatin-induced cognitive impairment in rats and improves hippocampal dendritic spine density. NeuroReport. 2024; 35: 657–663. https://doi.org/10.1097/wnr.0000000000002049

[10] Chao OY, Nikolaus S, Yang YM, Huston JP. Neuronal circuitry for recognition memory of object and place in rodent models. Neuroscience and Biobehavioral Reviews. 2022; 141: 104855. https://doi.org/10.1016/j.neubiorev.2022.104855

[11] Waters SJ, Basile BM, Murray EA. Reevaluating the role of the hippocampus in memory: A meta-analysis of neurotoxic lesion studies in nonhuman primates. Hippocampus. 2023; 33: 787–807. https://doi.org/10.1002/hipo.23499

[12] Huston JP, Chao OY. Probing the nature of episodic memory in rodents. Neuroscience and Biobehavioral Reviews. 2023; 144: 104930. https://doi.org/10.1016/j.neubiorev.2022.104930

[13] Csik B, Vali Kordestan K, Gulej R, Patai R, Nyul-Toth A, Shanmugarama S, et al. Cisplatin and methotrexate induce brain microvascular endothelial and microglial senescence in mouse models of chemotherapy-associated cognitive impair-

ment. GeroScience. 2025; 47: 3447–3459. https://doi.org/10.1007/s11357-025-01560-6

[14] Patai R, Csik B, Nyul-Toth A, Gulej R, Vali Kordestan K, Chandragiri SS, et al. Persisting blood–brain barrier disruption following cisplatin treatment in a mouse model of chemotherapy-associated cognitive impairment. GeroScience. 2025; 47: 3835–3847. https://doi.org/10.1007/s11357-025-01569-x

[15] Goyal A, Agrawal A, Verma A, Dubey N. The PI3K-AKT pathway: A plausible therapeutic target in Parkinson's disease. Experimental and Molecular Pathology. 2023; 129: 104846. https://doi.org/10.1016/j.yexmp.2022.104846

[16] Sánchez-Castillo C, Cuartero MI, Fernández-Rodrigo A, Briz V, López-García S, Jiménez-Sánchez R, et al. Functional specialization of different PI3K isoforms for the control of neuronal architecture, synaptic plasticity, and cognition. Science Advances. 2022; 8: eabq8109. https://doi.org/10.1126/sciadv.abq8109

[17] Khakha N, Khan H, Kaur A, Singh TG. Therapeutic implications of phosphorylation- and dephosphorylation-dependent factors of cAMP-response element-binding protein (CREB) in neurodegeneration. Pharmacological Reports: PR. 2023; 75: 1152–1165. https://doi.org/10.1007/s43440-023-00526-9

[18] Mahmoud AM, Mantawy EM, Wahdan SA, Ammar RM, El-Demerdash E. Vildagliptin restores cognitive function and mitigates hippocampal neuronal apoptosis in cisplatin-induced chemo-brain: Imperative roles of AMPK/Akt/CREB/BDNF signaling cascades. Biomedicine & Pharmacotherapy. 2023; 159: 114238. https://doi.org/10.1016/j.biopha.2023.114238

[19] Zhang Y, Ren Y, Chen X, Deng S, Lu W. Role of Butylphthalide in Immunity and Inflammation: Butylphthalide May Be a Potential Therapy for Anti-Inflammation and Immunoregulation. Oxidative Medicine and Cellular Longevity. 2022; 2022: 7232457. https://doi.org/10.1155/2022/7232457

[20] Gao Y, Hu M, Niu X, Li M, Xu L, Xiao Y, et al. Dl-3-n-Butylphthalide Improves Neuroinflammation in Mice with Repeated Cerebral Ischemia-Reperfusion Injury through the Nrf2-Mediated Antioxidant Response and TLR4/MyD88/NF-κB Signaling Pathway. Oxidative Medicine and Cellular Longevity. 2022; 2022: 8652741. https://doi.org/10.1155/2022/8652741

[21] Che P, Zhang J, Yu M, Tang P, Wang Y, Lin A, et al. Dl-3-n-butylphthalide promotes synaptic plasticity by activating the Akt/ERK signaling pathway and reduces the blood-brain barrier leakage by inhibiting the HIF-1α/MMP signaling pathway in vascular dementia model mice. CNS Neuroscience & Therapeutics. 2023; 29: 1392–1404. https://doi.org/10.1111/cns.14112

[22] Yan L, Gu L, Lv X, Ni Z, Qian W, Chen Z, et al. Butylphthalide mitigates traumatic brain injury by activating anti-ferroptotic AHR-CYP1B1 pathway. Journal of Ethnopharmacology. 2025; 337: 118758. https://doi.org/10.1016/j.jep.2024.118758

[23] Zhang H, Wang L, Yang Y, Cai C, Wang X, Deng L, et al. DL-3-n-butylphthalide (NBP) alleviates poststroke cognitive impairment (PSCI) by suppressing neuroinflammation and oxidative stress. Frontiers in Pharmacology. 2023; 13: 987293. https://doi.org/10.3389/fphar.2022.987293

[24] Yao M, Wen M, Huang Z, Chen P, Zhou B. The effect of butylphthalein regulating the PI3K/Akt/CREB signaling pathway on cisplatin-induced inflammation and apoptosis in PC12 cells. Yaoxue Qianyan Zazhi. 2025; 29: 721–729. https://doi.org/10.12173/j.issn.2097-4922.202502073 (In Chinese)

[25] Wang XL, Lin FL, Xu W, Wang C, Wang QQ, Jiang RW. Silybin B exerts protective effect on cisplatin-induced neurotoxicity by alleviating DNA damage and apoptosis. Journal of Ethnopharmacology. 2022; 288: 114938. https://doi.org/10.1016/j.jep.2021.114938

[26] Zhou W, Kavelaars A, Heijnen CJ. Metformin Prevents Cisplatin-Induced Cognitive Impairment and Brain Damage in Mice. PloS One. 2016; 11: e0151890. https://doi.org/10.1371/journal.pone.0151890

[27] Chong Z, Feng Y. dl-3-n-butylphthalide reduces brain damage in mice with closed head injury. Chinese medical journal. 2000; 113: 613–616.

[28] Zhao Y, Lee JH, Chen D, Gu X, Caslin A, Li J, et al. DL-3-n-butylphthalide induced neuroprotection, regenerative repair, functional recovery and psychological benefits following traumatic brain injury in mice. Neurochemistry International. 2017; 111: 82–92. https://doi.org/10.1016/j.neuint.2017.03.017

[29] Alhowail AH. Cisplatin induces hippocampal neurotoxicity and cognitive impairment in rats through neuroinflammation, oxidative stress, and overexpression of glutamatergic receptors mRNA. Frontiers in Pharmacology. 2025; 16: 1592511. https://doi.org/10.3389/fphar.2025.1592511

[30] Hassan MAM, Wahdan SA, El-Naga RN, Abdelghany TM, El-Demerdash E. Ondansetron attenuates cisplatin-induced behavioral and cognitive impairment through downregulation of NOD-like receptor inflammasome pathway. Toxicology and Applied Pharmacology. 2024; 485: 116875. https://doi.org/10.1016/j.taap.2024.116875

[31] Sun M, Chen J, Liu F, Li P, Lu J, Ge S, et al. Butylphthalide inhibits ferroptosis and ameliorates cerebral Ischaemia-Reperfusion injury in rats by activating the Nrf2/HO-1 signalling pathway. Neurotherapeutics: the Journal of the American Society for Experimental NeuroTherapeutics. 2024; 21: e00444. https://doi.org/10.1016/j.neurot.2024.e00444

[32] Li S, Zhao J, Xi Y, Ren J, Zhu Y, Lu Y, et al. Dl-3-n-butylphthalide exerts neuroprotective effects by modulating hypoxia-inducible factor 1-alpha ubiquitination to attenuate oxidative stress-induced apoptosis. Neural Regeneration Research. 2023; 18: 2424–2428. https://doi.org/10.4103/1673-5374.371366

[33] Murillo LC, Sutachan JJ, Albarracín SL. An update on neurobiological mechanisms involved in the development of chemotherapy-induced cognitive impairment (CICI). Toxicology Reports. 2023; 10: 544–553. https://doi.org/10.1016/j.toxrep.2023.04.015

[34] Grant CV, Sullivan KA, Wentworth KM, Otto LD, Strehle LD, Otero JJ, et al. Microglia are implicated in the development of paclitaxel chemotherapy-associated cognitive impairment in female mice. Brain, Behavior, and Immunity. 2023; 108: 221–232. https://doi.org/10.1016/j.bbi.2022.12.004

[35] Patani R, Hardingham GE, Liddelow SA. Functional roles of reactive astrocytes in neuroinflammation and neurodegeneration. Nature Reviews. Neurology. 2023; 19: 395–409. https://doi.org/10.1038/s41582-023-00822-1

[36] Paolicelli RC, Sierra A, Stevens B, Tremblay ME, Aguzzi A, Ajami B, et al. Microglia states and nomenclature: A field at its crossroads. Neuron. 2022; 110: 3458–3483. https://doi.org/10.1016/j.neuron.2022.10.020

[37] Matusova Z, Hol EM, Pekny M, Kubista M, Valihrach L. Reactive astrogliosis in the era of single-cell transcriptomics. Frontiers in Cellular Neuroscience. 2023; 17: 1173200. https://doi.org/10.3389/fncel.2023.1173200

[38] Wang Z, Wang J, Yun J, Song J, Chen Q, Wang D, et al. Effectiveness of DL-3-n-butylphthalide in the treatment of poststroke cognitive impairment and its associated predictive cytokines: a systematic review and meta-analysis. BMC Pharmacology and Toxicology. 2024; 25: 65. https://doi.org/10.1186/s40360-024-00793-z

[39] Zhou Q, Han C, Xia Y, Wan F, Yin S, Li Y, et al. Efficacy and safety of 3-n-butylphthalide for the treatment of cognitive impairment: A systematic review and meta-analysis. CNS Neuroscience & Therapeutics. 2022; 28: 1706–1717. https://doi.org/10.1111/cns.13952

[40] Ge M, Jin L, Cui C, Han Y, Li H, Gao X, et al. Dl-3-n-butylphthalide improves stroke outcomes after focal ischemic stroke in mouse model by inhibiting the pyroptosis-regulated cell death and ameliorating neuroinflammation. European Journal of Pharmacology. 2024; 974: 176593. https://doi.org/10.1016/j.ejphar.2024.176593

[41] Xu S, Li X, Li Y, Li X, Lv E, Zhang X, et al. Neuroprotective effect of Dl-3-n-butylphthalide against ischemia–reperfusion injury is mediated by ferroptosis regulation via the SLC7A11/GSH/GPX4 pathway and the attenuation of blood–brain barrier disruption. Frontiers in Aging Neuroscience. 2023; 15: 1028178. https://doi.org/10.3389/fnagi.2023.1028178

[42] Lu J, Zhang J, Wang X, Yuan F, Xin B, Li J, et al. Dl-3-n-butylphthalide promotes microglial phagocytosis and inhibits microglial inflammation via regulating AGE-RAGE pathway in APP/PS1 mice. Brain Research Bulletin. 2024; 212: 110969. https://doi.org/10.1016/j.brainresbull.2024.110969

[43] Fowler CG, Tarantino MI, Gillett AE, Muñiz V, Anderson MA, Bonner RL, et al. Using a murine model to explore the impact of sex and APOE4 on cisplatin-induced cognitive impairment. Brain, Behavior, and Immunity. 2025; 129: 1–14. https://doi.org/10.1016/j.bbi.2025.05.010

[44] Peng Y, Wang Y, Zhou C, Mei W, Zeng C. PI3K/Akt/mTOR Pathway and Its Role in Cancer Therapeutics: Are We Making Headway? Frontiers in Oncology. 2022; 12: 819128. https://doi.org/10.3389/fonc.2022.819128

[45] Jiang Q, Zhang N, Li X, Hou W, Zhao XQ, Liu L. Dl-3-N-Butylphthalide Presents Anti-Cancer Activity in Lung Cancer by Targeting PD-1/PD-L1 Signaling. Cancer Management and Research. 2021; 13: 8513–8524. https://doi.org/10.2147/cmar.s333416

[46] Tang AL, Liu XY, Gao N, Hu TP, Yan ST, Zhang GQ. Dl-3-n-butylphthalide improves intestinal microcirculation disorders in septic rats by regulating the PI3K/AKT signaling pathway and autophagy. International Immunopharmacology. 2023; 118: 110049. https://doi.org/10.1016/j.intimp.2023.110049